表2 難聴児の発達・療育・教育についての7つの誤解

1．先天性難聴児には喃語がない。したがって喃語があれば難聴はない。

間違いである。先天性難聴児も初期の喃語は健聴児と同様に活発にある。

2．難聴児通園施設はスパルタ式の怖いところである。

間違いである。母親も子どもも楽しみにして通園し，将来の希望がある。大学への進学率が60%に近い。

3．ろう学校は手話教育しかしない。

間違いである。私立日本聾話学校と国立筑波大学附属聴覚特別支援学校（筑波大学附属聾学校）は聴覚口話に手話を併用している。公立ろう学校は聴覚口話と手話を併用する。

4．人工内耳はメスを使っているので危険である。

間違いである。素人がメスを振り回せば危険であるが，耳の外科医が使う限り安全で，病気を治すことができる。外科手術をすでに500年の歴史がある。

メスを使って治療しなければ治すことができない病気はたくさんある。

5．人工内耳は将来手術をやり直さなければならない。スピーチプロセッサーも新型に変えなければならない。そのときにまた100万円もの費用がかかる。

間違いである。事故で人工内耳が故障した場合は特定医療材料費という援助する仕組みがある。1996年に保険に適用されて以来，14年が過ぎたが，自然な故障は100件中数件にすぎない。スピーチプロセッサーの破損は病院で健康保険の特定医療材料費という制度により保険の範囲で供給される。

6．難聴児は大学へ行く者がまれである。

間違いである。東京の難聴児通園施設に通った補聴器装用で成長した青年の60%，私立ろう学校では50%が大学へ進学している。カナダのモントリオールの聴覚口話学校は人工内耳と補聴器で育った80%が大学へ進学しているほど進学率が高い。

7．聴覚口話の教育施設は手話を絶対に使用させない偏ったところである。

間違いである。日本人の母語は日本語である。その日本語も最初に正しく聴いて話し，書く力は聴覚口話で脳の可塑性の豊かな乳幼児期には習得して，日本語が確立してから手話を学ぶことが勧められる。その方が成人して社会で活躍するときに有用である。手話には助詞や接続詞がないため，手話だけの教育を受けると助詞がうまく使えないことがあり，誤解されることが多い。

両耳に補聴器を装用し，以下のところで就学前の教育を受けます（表1）。

①聴児通園施設（全国で27ある。児童福祉法によるもので厚生労働省管轄）

②地域の身障センター・療育センターなどが（全国に多数ある。地域の地方自治体管轄）

③ろう学校（全国に102ある。学校教育法によるもので，文部科学省の管轄）

a．私立日本聾話学校(聴覚口話)

b．国立筑波大学附属聴覚特別支援学校(筑波大学附属聾学校)(文部科学省管轄。聴覚口話)

c．公立ろう学校（都道府県立，市立。聴覚口話・日本語対応手話併用）

d．私立明晴学園（日本手話）

どこでも初めは補聴下に教育を受けますが，難聴が重度の場合は，1歳半以降に人工内耳手術を受けて聴覚口話法教育を受けます。

小学・中学の義務教育期間はどこで教育を受けますか？

①普通小・中学校（私立・公立）

②難聴児学級を併設する普通小・中学校（公立）

③ろう学校

a．私立日本聾話学校

b．国立筑波大学附属聴覚特別支援学校(筑波大学附属聾学校)

c．公立ろう学校

高校教育はどこで教育を受けますか？

①普通高校（私立・公立）

②ろう学校高等部

大学教育はどこで教育を受けますか？

①一般の大学
②筑波技術大学

社会に出るときに会社の方の配慮がありますか？

企業の障害者枠を利用して入社する場合があります。

おわりに

先天性難聴児の場合，早期発見・早期教育がわが国でも定着し，補聴器だけでなく人工内耳もあり，大いに希望の持てる時代となりました。それにもかかわらずここで述べたことが理解されていないために本来受けるべき早期のサービスや教育が手遅れとなる「不都合な現実」があります。教育方法が異なると，まるで宗教間の対立に類似した現実があり，これを7つの誤解として表2にまとめましたのでご参照ください。

成長してから教育をやり直すことはできません。言語の習得は，脳の可塑性（かそせい）の時期がすぎると手遅れになります。自分の歩んだ道を肯定的に考えるほかなくなるのです。

●文献●

1) 加我君孝，編：新生児聴覚スクリーニング 早期発見・早期教育のすべて．金原出版，2005
2) 大沼直紀：日本における障害教育の展望と課題．韓国聴覚口話教育 100 周年記念誌．pp77-93，2009

☆☆☆☆☆ ☆☆☆☆☆

Jpn J Ophthalmol
DOI 10.1007/s10384-012-0126-7

CLINICAL INVESTIGATION

Survey of microphthalmia in Japan

Sachiko Nishina · Daijiro Kurosaka · Yasuhiro Nishida · Hiroyuki Kondo · Yuri Kobayashi · Noriyuki Azuma

Received: 17 May 2011 / Accepted: 17 January 2012

Abstract
Purpose To report the current status of patients with microphthalmia based on a cross-sectional survey of patient hospital visits.
Methods A questionnaire was sent to the departments of ophthalmology in 1,151 major Japanese hospitals to survey the following: the number of patients with microphthalmia who visited the outpatient clinics between January 2008 and December 2009; gender; age; family history; associated ocular anomalies; complications and systemic diseases; surgical treatment; vision and management. A retrospective quantitative registry of 1,254 microphthalmic eyes (851 patients) from 454 hospitals (39.4%) was compiled.
Results Of the patients for whom data were available, 50% ranged in age from 0 to 9 years. The major ocular findings were nanophthalmos, coloboma, and vitreoretinal malformations. Ocular complications frequently developed, including cataracts, glaucoma, and retinal detachment. Surgery was performed in 21.4% of all cases, and systemic diseases were present in 31% of all cases. The vision associated with microphthalmia exceeded 0.1 in about 30% of the eyes. Glasses and low vision aids were used by 21.6% of patients.
Conclusions Patients with microphthalmia often have ocular and systemic anomalies. Early assessment and preservation of vision and long-term complication management are needed.

Keywords Microphthalmos · Epidemiology · Survey · Intractable disease

S. Nishina (✉) · Y. Kobayashi · N. Azuma
Division of Ophthalmology, National Center for Child Health and Development, 2-10-1 Okura, Setagaya-ku, Tokyo 157-8535, Japan
e-mail: nishina-s@ncchd.go.jp

D. Kurosaka
Department of Ophthalmology, Iwate Medical University School of Medicine, Iwate, Japan

Y. Nishida
Department of Ophthalmology, Shiga University of Medical Science, Shiga, Japan

H. Kondo
Department of Ophthalmology, University of Occupational and Environmental Health, Japan, Fukuoka, Japan

Introduction

Microphthalmos is defined as the arrested development of all global dimensions and is often is associated with other ocular and systemic anomalies [1]. Chromosomal disorders, genetic syndromes, and environmental factors, such as maternal infection and exposure to X-rays or drugs, are reported as causes [2]. However, in most cases the precise pathogenesis is unknown although some causative genes (*SOX2* and *PAX6*) have been identified [2–4].

Previous studies conducted in the UK report that the prevalence rates of microphthalmia, anophthalmia, and typical coloboma are 10–19 per 100,000 births [4–7]. Microphthalmia is rare, and only a few disease, genetic, and epidemiologic studies and a few reports on the practical patient status have been published. The condition generally causes substantial visual impairment, but standard management and treatments have not been established.

We conducted a cross-sectional national survey to investigate the current status of patients with microphthalmia, focusing especially on ocular associations,

Published online: 23 February 2012

complications, surgery, and vision examinations performed by ophthalmologists.

Materials and methods

A questionnaire was sent to the departments of ophthalmology in 1,151 major hospitals nationwide, all of which are authorized by the Japanese Ophthalmological Society as training institutions for physicians specializing in ophthalmology, to survey the number of patients with microphthalmia who visited their outpatient clinics between January 2008 and December 2009. Patients referred to other hospitals during this period were excluded.

The diagnostic criterion for pure microphthalmos is the presence of an eye with two-thirds the normal ocular volume, i.e., 0.87 below the normal axial length [1]. The Japanese criteria were established by Majima [8], based on the average axial length for each age group of Japanese patients. The clinical definition can be determined by a substantial size difference between the two eyes. Axial lengths of <21 mm in adults and <19 mm in 1-year-old children, i.e., two standard deviations below normal, are used. Corneal diameters of <10 mm in adults and <9 mm in infants are used for a simple diagnosis [9]. In our survey, either Majima's criteria for pure microphthalmos or the clinical definition for complicated microphthalmos was applied.

The questionnaire asked for either the numbers of patients or the number of eyes and was divided into two sheets. The first sheet comprised questions on the number of cases, the number of cases operated on, whether the condition was unilateral or bilateral, gender, age, family history; the second sheet consisted of questions about the number of associated ocular anomalies and complications, surgical treatment, associated systemic diseases, vision and management with glasses, low vision aid, and the use of a prosthetic shell.

A retrospective quantitative registry of microphthalmia was compiled from the responses from 454 hospitals (39.4%). The data from 1,254 microphthalmic eyes of 851 cases in total were collected from the first sheet, but as some hospitals did not complete the second sheet, only data from 1,069 eyes of 722 cases were collected from the second sheet. Of the data collected for these 1,069 eyes, data on the vision of 56 eyes (5.2%) were incomplete. Thus, data from 1,013 eyes were analyzed for vision.

We surveyed the number of patients managed in Japanese hospitals and analyzed the associated ocular anomalies and complications, surgical treatment, systemic diseases, vision and ophthalmic management.

Results

Of the 851 cases [396 (46.5%) male, 455 (53.5%) female] of microphthalmia reported on the first sheet, 444 (52%) were unilateral and 405 (48%) were bilateral (for two cases no information on unilateralism or bilateralism was reported). In terms of age distribution, 50% of the patients were 0–9 years and 16% were 10–19 years; between ages 20 and 79 years, the prevalence remained relatively constant, ranging between 4.3 and 6.8% (Fig. 1). Family histories were positive in 61 cases (7.2%), of which 25 cases (41%) of autosomal dominant inheritance, three cases of X-linked recessive inheritance, and one case of autosomal recessive inheritance were identified; the other 32 cases were undetermined.

The data from the 1,069 microphthalmic eyes of 722 cases retrieved from the second sheet were compiled and analyzed for associated ocular anomalies and complications, surgical treatment, associated systemic diseases, and management with glasses, low vision aids, and prosthetic shells. The ocular abnormalities and complications associated with microphthalmia are shown in Fig. 2. The identified ocular findings were nanophthalmos, coloboma (choroid, retina, lens, iris), vitreoretinal malformation (retinal dysplasia, retinal fold, persistent fetal vasculature, etc.), anophthalmos/extreme microphthalmos, anterior segment dysgenesis (Peters' anomaly, aniridia), and optic

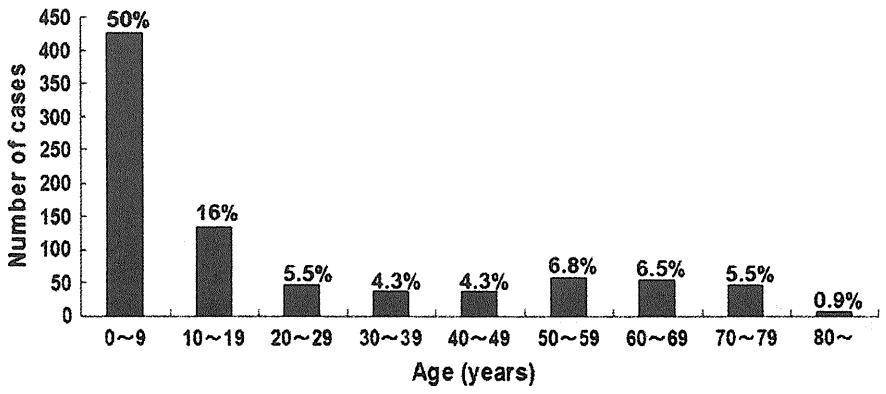

Fig. 1 Ages of patients with microphthalmia managed in the surveyed hospitals. The rate is given for each age group ($N = 851$ cases)

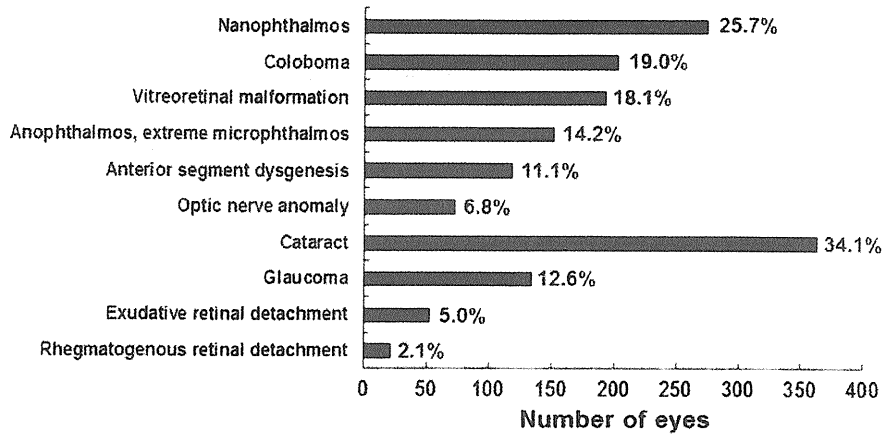

Fig. 2 Ocular abnormalities and complications associated with microphthalmia. The rate of each associated anomaly or complication is given ($N = 1{,}069$ eyes)

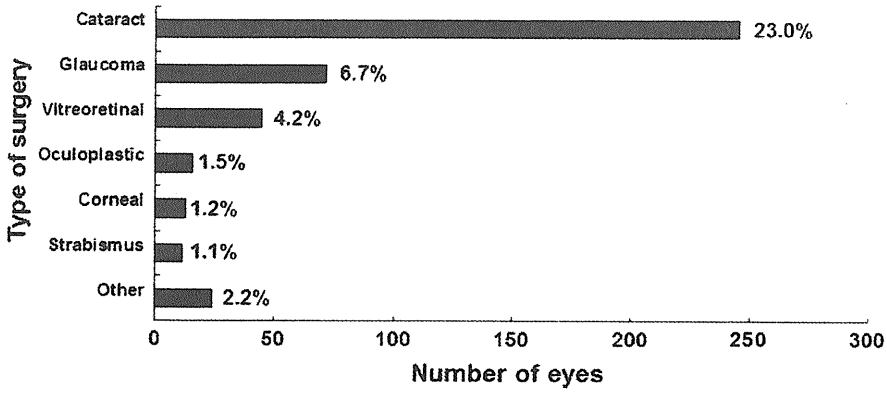

Fig. 3 Surgical treatments for ocular complications in microphthalmia. The rate of each surgical procedure is given ($N = 1{,}069$ eyes)

nerve anomaly (disc anomaly, optic nerve hypoplasia). The most frequent ocular complications were cataracts in 34.1%, followed by glaucoma and exudative or rhegmatogenous retinal detachment.

Surgery had been performed in 182 (21.4%) of the 851 cases; the surgical procedures for ocular complications are shown in Fig. 3. The procedures performed the most often were cataract extraction in 246 eyes (23.0%) of 1,069 eyes, followed by glaucoma surgery and vitreoretinal surgery.

Systemic diseases were present in 224 patients (31%) of 722 cases of microphthalmia, with 92 cases (12.7%) of developmental cerebral anomalies and mental deficiency, 68 cases (9.4%) of multiple anomalies and genetic syndromes, 26 cases (3.6%) of chromosomal disorders, and 38 cases (5.3%) of others.

The distribution of vision in microphthalmia is shown in Fig. 4. The data from 1,013 microphthalmic eyes were analyzed for vision. The visual acuity (VA) in microphthalmos was <0.02 in 348 eyes (34.4%), <0.1 but not <0.02 in 116 eyes (11.4%), <0.3 but not <0.1 in 93 eyes (9.2%), not <0.3 in 157 eyes (15.5%), unmeasurable with poor visual performance in 241 eyes (23.8%), and good visual performance in 58 eyes (5.7%).

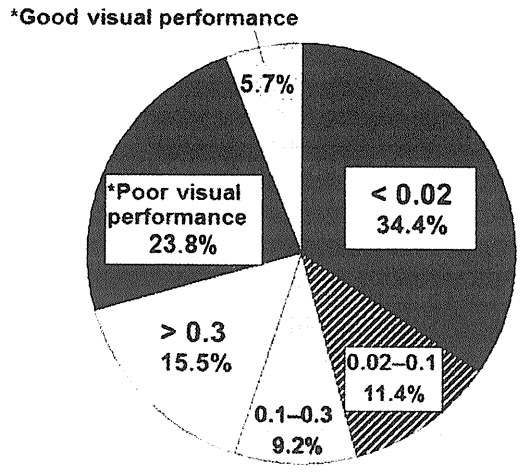

Fig. 4 Visual acuity (VA) in microphthalmos. *Asterisk* VA not measured due to young age or mental retardation. The rate of each VA group is given ($N = 1{,}013$ eyes)

Glasses and low vision aids were used in 156 cases (21.6%) of 722 cases, while prosthetic shells were applied in 211 eyes (19.7%) of 1,069 eyes.

Discussion

This is the first national survey that reports the epidemiologic aspects and current status of patients with microphthalmia in Japan. It is also the largest survey conducted by ophthalmologists of patients with microphthalmia who present at a hospital. The results based on cross-sectional surveys of patients' hospital visits may be considerably biased and may not be comparable with those of previous epidemiologic studies in other countries. However, the results of this survey showing the precise ocular associations, complications, types of surgeries, and vision, may be useful for future ocular management and investigation.

Approximately one-half of the patients in this survey who presented to a hospital were children under the age of 10 years, indicating that diagnosis and treatment of microphthalmia during the period of visual development are both needed and common practice in Japan. In addition, continuous management of low vision and ocular complications is required in order to maintain proper vision throughout life. Among the responders in this study, the distribution of microphthalmia was evenly divided between men and women and between unilateral cases and bilateral cases. Previous studies also report no biased association between microphthalmia and gender; however, those on laterality are mixed, with bilateral being more common in some studies and unilateral cases being more common in others [10]. Kallen et al. [11] reported that among their patient population, >70% of microphthalmia cases were bilateral and associated with chromosomal disorders, 53–60% were either associated or not associated with other malformations, but only 27% were cases of isolated microphthalmia. Microphthalmos associated with systemic diseases, nanophthalmos, colobomatous microphthalmos, and some cases of complicated microphthalmos often develop bilaterally and need more medical management for low vision and periodic follow-up. However, the current survey indicated that unilateral cases also require ophthalmic treatment and management.

The family histories were positive in 7.2% of cases; however, most cases have not been investigated for genetic etiology. To clarify the pathogenesis of various microphthalmia and develop useful treatments, effective genetic screening should be performed.

The current patient population had varying kinds and degrees of ocular-associated anomalies; among these, posterior segment dysgenesis, including coloboma and vitreoretinal malformations, was seen frequently. Thus, early morphologic and electrophysiologic evaluation of the posterior segment may be required to assess the visual potential and indications for surgical, optical, and amblyopia treatment or for a cosmetic shell.

The rates of developing cataracts, glaucoma, and retinal detachments were extremely high among the young patients. These ocular complications were major indications for surgical intervention, although the prognoses were generally poor [12]. Patients with microphthalmia require lifelong management for early prevention and detection of these complications. A less invasive surgical procedure for microphthalmia should be developed [13–19].

Various systemic anomalies are frequently associated with microphthalmia, indicating that initial assessment and continuous management by pediatricians are essential. Although 31% of the cases in our survey were microphthalmia associated with systemic disease, analysis of a population-based birth defects registry in Hawaii from 1986 to 2001 revealed that only 5% of the 96 cases had either isolated anophthalmia or microphthalmia, whereas 25% had confirmed chromosomal abnormalities, such as trisomy 18 and 13, and others had malformation syndromes, limb and musculoskeletal system defects, and cardiac and circulatory system defects [10]. Our survey included more unilaterally isolated cases, probably because ophthalmologists conducted the survey and provided detailed descriptions of the ocular status of the patients who presented to the hospitals.

Overall useful vision and good visual performance >0.1 were obtained in about 30% of microphthalmia cases, whereas about 34% of microphthalmia patients were blind (VA <0.02). However, glasses and low vision aids were used in around 22% of the cases, while prosthetic shells were used in about 20% of eyes. The visual prognosis of microphthalmos depends largely on the difference between the two eyes. The chances of obtaining good VA are limited in cases of severe unilateral microphthalmos, where orbital growth may be retarded and facial deformity may develop. Early socket expansion and wearing of a prosthetic shell are important for cosmetic treatment in anophthalmos and extreme microphthalmos [20]. However, microphthalmos with visual potential should be assessed early and glasses prescribed to maximize the VA.

In summary, our analysis of the survey data revealed that patients with microphthalmia have various ocular and systemic anomalies and that the rates of ocular complications are high in young patients. Early assessment, preservation of vision, and long-term management of complications are needed for these patients.

Acknowledgments The authors wish to thank all ophthalmologists in the 454 participating hospitals for their collaboration with this survey. This study was supported by Health and Labour Sciences Research Grants of Research on intractable diseases from the Ministry of Health, Labour and Welfare, Tokyo, Japan.

References

1. Duke-Elder S. Microphthalmos. In: Duke-Elder S, editor. System of ophthalmology, vol III. Normal and abnormal development,

part 2. Congenital deformities. London: Henry Kimpton; 1964. p. 488–95.
2. Verma AS, Fitzpatrick DR. Anophthalmia and microphthalmia. Orphanet J Rare Dis. 2007;2:47.
3. Hever AM, Williamson KA, van Heyningen V. Developmental malformations of the eye: the role of *PAX6, SOX2* and *OTX2*. Clin Genet. 2006;69:459–70.
4. Morrison D, FitzPatrick D, Hanson I, Williamson K, van Heyningen V, Fleck B, et al. National study of microphthalmia, anophthalmia, and coloboma (MAC) in Scotland: investigation of genetic aetiology. J Med Genet. 2002;39:16–22.
5. Dolk H, Busby A, Armstrong BG, Walls PH. Geographical variation in anophthalmia and microphthalmia in England, 1988–94. Br Med J. 1998;317:905–9.
6. Busby A, Dolk H, Collin R, Jones RB, Winter R. Compiling a national register of babies born with anophthalmia/microphthalmia in England 1988–94. Arch Dis Child Fetal Neonatal Ed. 1998;79:F168–73.
7. Shah SP, Taylor AE, Sowden JC, Ragge NK, Russell-Eggitt I, Rahi JS, et al. Anophthalmos, microphthalmos and typical coloboma in the UK: a prospective study of incidence and risk. Invest Ophthalmol Vis Sci. 2011;52:558–64.
8. Majima A. Microphthalmos and its pathogenic classification (in Japanese with English abstract). Nippon Ganka Gakkai Zasshi (J Jpn Ophthalmol Soc). 1994;98:1180–200.
9. Weiss AH, Kousseff BG, Ross EA, Longbottom J. Complex microphthalmos. Arch Ophthalmol. 1989;107:1619–24.
10. Forrester MB, Merz RD. Descriptive epidemiology of anophthalmia and microphthalmia, Hawaii, 1986–2001. Birth Defect Res A Clin Mol Teratol. 2006;76:187–92.
11. Kallen B, Robert E, Harris J. The descriptive epidemiology of anophthalmia and microphthalmia. Int J Epidemiol. 1996;25:1009–16.
12. Singh OS, Simmons RJ, Brockhurst RJ, Trempe CL. Nanophthalmos: a perspective on identification and therapy. Ophthalmology. 1982;89:1006–12.
13. Yu SY, Lee JH, Chang BL. Surgical management of congenital cataract associated with severe microphthalmos. J Cataract Refract Surg. 2000;26:1219–24.
14. Nishina S, Noda E, Azuma N. Outcome of early surgery for bilateral congenital cataracts in eyes with microcornea. Am J Ophthalmol. 2007;144:276–80.
15. Vasavada VA, Dixit NV, Ravat FA, Praveen MR, Shah SK, Vasavada V, et al. Intraoperative performance and postoperative outcome of cataract surgery in infant eyes with microphthalmos. J Cataract Refract Surg. 2009;35:519–28.
16. Brockhurst RJ. Cataract surgery in nanophthalmic eyes. Arch Ophthalmol. 1990;108:965–7.
17. Wu W, Dawson DG, Sugar A, Elner SG, Meyer KA, McKey JB, et al. Cataract surgery in patients with nanophthalmos: results and complications. J Cataract Refract Surg. 2004;30:584–90.
18. Wladis EJ, Gewirtz MB, Guo S. Cataract surgery in the small adult eye. Surv Ophthalmol. 2006;51:153–61.
19. Kocak I, Altintas AG, Yalvac IS, Nurozler A, Kasim R, Duman S. Treatment of glaucoma in young nanophthalmic patients. Int Ophthalmol. 1997;20:107–11.
20. Ragge NK, Subak-Sharpe ID, Collin JRO. A practical guide to the management of anophthalmia and microphthalmia. Eye. 2007;21:1290–300.

Human Molecular Genetics, 2011, Vol. 20, No. 23 **4530–4539**
doi:10.1093/hmg/ddr394
Advance Access published on September 7, 2011

Modeling familial Alzheimer's disease with induced pluripotent stem cells

Takuya Yagi[1], Daisuke Ito[1,*], Yohei Okada[2,3], Wado Akamatsu[2], Yoshihiro Nihei[1], Takahito Yoshizaki[1], Shinya Yamanaka[4], Hideyuki Okano[2] and Norihiro Suzuki[1]

[1]Department of Neurology, [2]Departments of Physiology and [3]Kanrinmaru Project, School of Medicine, Keio University, 35 Shinanomachi, Shinjuku-ku, Tokyo 160-8582, Japan and [4]Center for iPS Cell Research and Application, Kyoto University, Kyoto 606-8507, Japan

Received June 3, 2011; Revised August 1, 2011; Accepted August 29, 2011

Alzheimer's disease (AD) is the most common form of age-related dementia, characterized by progressive memory loss and cognitive disturbance. Mutations of presenilin 1 (*PS1*) and presenilin 2 (*PS2*) are causative factors for autosomal-dominant early-onset familial AD (FAD). Induced pluripotent stem cell (iPSC) technology can be used to model human disorders and provide novel opportunities to study cellular mechanisms and establish therapeutic strategies against various diseases, including neurodegenerative diseases. Here we generate iPSCs from fibroblasts of FAD patients with mutations in *PS1* (A246E) and *PS2* (N141I), and characterize the differentiation of these cells into neurons. We find that FAD–iPSC-derived differentiated neurons have increased amyloid β42 secretion, recapitulating the molecular pathogenesis of mutant presenilins. Furthermore, secretion of amyloid β42 from these neurons sharply responds to γ-secretase inhibitors and modulators, indicating the potential for identification and validation of candidate drugs. Our findings demonstrate that the FAD-iPSC-derived neuron is a valid model of AD and provides an innovative strategy for the study of age-related neurodegenerative diseases.

INTRODUCTION

Alzheimer's disease (AD) is one of the most common neurodegenerative disorders of the elderly, characterized by progressive memory disorientation and cognitive disturbance. The pathological profile of AD is neuronal loss in the cerebral cortex accompanied by massive accumulation of two types of amyloid fibril seeding senile plaques and hyperphosphorylated tau forming paired helical filaments. The amyloid fibril is mainly composed of β-amyloid (Aβ) peptides, the 40 and 42 amino acid forms (Aβ40 and Aβ42), that are derived by proteolytic cleavages from the amyloid precursor protein (APP) by β- and γ-secretase activity (1,2). According to the amyloid cascade hypothesis, a prevailing theory of AD pathology, accumulation of Aβ, mainly Aβ42, in the brain is the initiator of AD pathogenesis, subsequently leading to the formation of neurofibrillary tangles containing hyperphosphorylated tau protein, and consequently neuronal loss (3–5).

Presenilin 1 (*PS1*) and presenilin 2 (*PS2*) genes encoding the major component of γ-secretase have been identified as the causative genes for autosomal-dominant familial Alzheimer's disease (FAD). Mutations in the *PS1* gene, located on chromosome 14, occur most frequently in FAD (6,7). Ala246Glu (A246E) in *PS1* is a well-characterized FAD mutation that shows typical phenotypes of AD with complete penetrance. Mutations in the *PS2* gene on chromosome 1 are a relatively rare cause of FAD and are variably penetrant. Asn-141 substitutions by Ile (N141I) in the *PS2* gene was the first identified causative mutation of *PS2* in affected patients from the now famous Volga German families (8,9).

Mutations in the *PS1*, *PS2* and the *APP* gene account for most of the familial early onset cases of AD either by enhancing the production of pathological Aβ or especially Aβ42, which has a greater tendency to form fibrillary amyloid deposits. These findings support β-amyloid as the common initiating factor in AD in the amyloid cascade hypothesis (10,11). Both A246E in *PS1* and N141I in *PS2* are reported to induce

*To whom correspondence should be addressed at: Department of Neurology, School of Medicine, Keio University, 35 Shinanomachi, Shinjuku-ku, Tokyo 160-8582, Japan. Tel: +81 353633788; Fax: +81 333531272; Email: d-ito@jk9.so-net.ne.jp

elevation of Aβ42 levels in human plasma, patient-derived fibroblasts, forced-expressed cells and, in mice, showing strong toxicity (10–13).

Generation of human iPSCs provides a new method for elucidating the molecular basis of human disease (14,15). An increasing number of studies have employed disease-specific human iPSCs in neurological diseases, and a few have demonstrated disease-specific phenotypes to model the neurological phenotype (16–24). Here, we report the generation of iPSC from fibroblasts of FAD with the *PS1* mutation A246E and the *PS2* mutation N141I, and differentiation of these cells into neurons. We demonstrate that patient-derived differentiated neurons increase Aβ42 secretion, recapitulating the pathological mechanism of FAD with *PS1* and *PS2* mutations. Our findings demonstrate that the FAD–iPSC-derived neuron is a valid model for studying AD, and provides important clues for the identification and validation of candidate drugs.

RESULTS

Generation of iPSC with presenilin mutations

We established two clones of iPSCs with the *PS1* mutation, A246E (PS1-2 iPSC and PS1-4 iPSC) and with the *PS2* mutation, N141I (PS2-1 iPSC and PS2-2 iPSC) by retroviral transduction of primary human fibroblasts with the five factors OCT4, SOX2, KLF4, LIN28 and NANOG. Fibroblasts were obtained from the Coriell Cell Repository (AG07768 and AG09908). The 201B7 iPSC line (14) and the sporadic Parkinson disease (PD)-derived iPSC lines (PD01-25 and 26) were reprogrammed by an original method (14) with four transcription factors (OCT4, SOX2, KLF4 and cMYC) and were used as the controls in this study. Genotyping of the established iPSC lines was confirmed by PCR–RFLP and sequencing (Fig. 1A and B). All PS1 and PS2 iPSC clones demonstrated typical characteristics of pluripotent stem cells: similar morphology to ESCs, expression of pluripotent markers including Tra-1-60, Tra-1-81, SSEA3 and SSEA4 (Fig. 1C), silencing of retroviral transgenes and reactivation of genes indicative of pluripotency (Fig. 1D). The differentiation ability of PS1 and PS2 iPSC was also confirmed *in vivo* by teratoma formation (Fig. 2), and *in vitro* by the formation of three germ layers via embryoid bodies (Supplementary Material, Fig. S1). To validate our reprogramming technique, we performed comprehensive analysis of two PS2 iPSCs. Heat map analysis showed that global gene expression profiles, including the critical genes for pluripotency, were similar between the iPSC lines established with four transcription factors (201B7 and PD01-25) and the PS2 iPSC clones established with five transcription factors (Supplementary Material, Fig. S2). In addition, there were no significant differences in the expression of AD-related molecules between PS2 iPSCs and control iPSCs (Supplementary Material, Fig. S3). Array comparative genomic hybridization (aCGH) analysis on PS2-1, PS2-2 iPSC and AG09908 fibroblasts showed that the total number of copy number aberrations were 52, 61 and 102 out of ~17 000 locations, respectively (Supplementary Material, Table S1), and no aberrations were detected in *APP*, *PS1* and *PS2* genes.

Differentiation of PS1 iPSC and PS2 iPSC into neurons

Differentiation of FAD patient-specific iPSCs towards neurons enables modeling the disease pathogenesis *in vitro*. To establish whether the presenilin mutations may affect neuronal differentiation, both PS1 and PS2 iPSC lines, as well as control iPSC lines, were induced to differentiate into neural cells (25,26), and cultured on Matrigel-coated dishes for 2 weeks to induce terminal differentiation (Fig. 3). We confirmed neuronal differentiation by the expression of neuronal markers, βIII-tubulin, and MAP-2 (Fig. 3A and B). As shown in Figure 3C. no obvious differences in the ability to generate neurons (~80% βIII-tubulin-positive cells) were observed among control, PS1 and PS2 iPSCs. This indicated that PS1 and PS2 iPSCs can generate neurons with almost the same efficiency as the control iPSCs, suggesting these presenilin mutations may have no significant effect on neuronal differentiation.

Production of Aβ secreted from iPSCs-derived neurons

To analyze the functional aspects of FAD, we investigated Aβ secretion from iPSC or iPSC-derived neurons. The Aβ secretion in the conditioned medium from control iPSC, PS1 iPSC and PS2 iPSC was very low; Aβ42 secretion especially was below the detection sensitivity. We therefore could not compare the ratio of Aβ42 to Aβ40 among iPSC lines. However, the Aβ secretion in the conditioned medium from the iPSCs-derived neurons was increased and measurable, indicating that Aβ secretion could undergo significant fluctuation during differentiation. Although the levels of Aβ42 and Aβ40 in the medium showed some clonal variation (Fig. 4A), possibly depending on the rate of cell growth and passage number, the ratio of Aβ42 to Aβ40 was significantly elevated in the PS1 and PS2 iPSCs-derived neurons, compared with the controls (Fig. 4B). Thus, PS1 and PS2 iPSCs show that living neurons derived from patients with the presenilin mutations ending at residue 42 that are linked to FAD secrete more Aβ. This result is compatible with previous evidences based on patients' plasma, fibroblasts and forced-expressed cells (10–13).

To explore recapitulation of key pathological events in AD, we investigated whether FAD-iPSC-derived differentiated neurons exhibit abnormal accumulation of tau and performed an immunoblot analysis of lysates of FAD-iPSC-derived neurons with anti-tau antibody. However, as shown in Supplementary Material, Figure S4, no abnormal tau protein accumulation or tangle formation was detected in the FAD-derived neurons, indicating that recapitulation of tauopathy is difficult to observe during the short culture period (2 weeks) in the present protocol.

Pharmacological response to γ-secretase inhibitors in PS1 iPSC- and PS2 iPSC-derived neurons

To evaluate the capacity of pharmacological drug screening in iPSC technology, we assessed whether inhibitors could affect the secretion of Aβ in PS1 and PS2 iPSCs-derived neurons. We first examined the secretion of Aβ from PS1-4 and PS2-2 iPSCs-derived neurons in the presence of Compound E, a

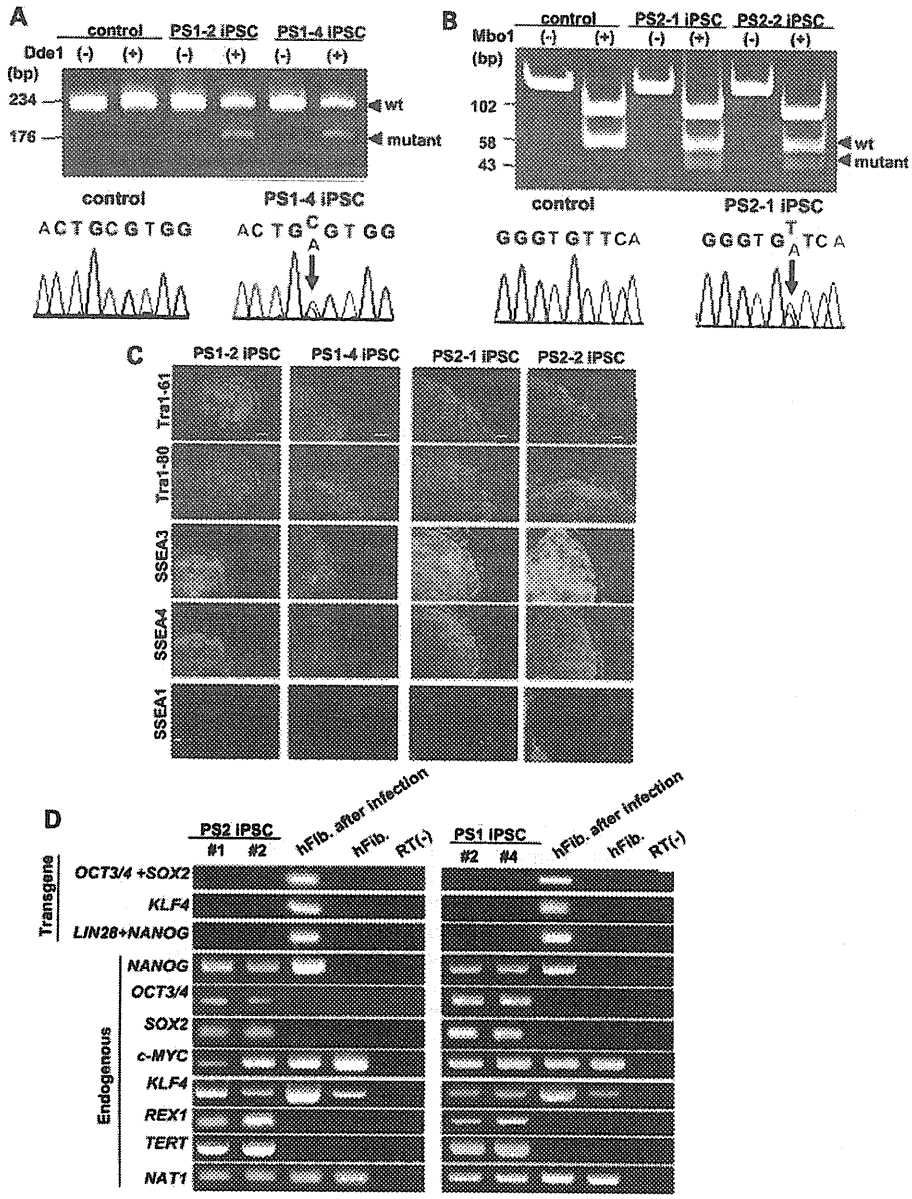

Figure 1. Generation of PS1 and PS2 iPSC from patient fibroblasts. (**A**) Genotypic analysis of PS1 iPSC by PCR–RFLP and sequencing. A246E genotyping by PCR–RFLP was performed with restriction enzyme *Dde*I. The A246E mutation results in fragments of 176 and 58 bp, whereas the control fragment has 234 bp. (**B**) Genotypic analysis of PS2 iPSC by PCR–RFLP and sequencing. N141I genotyping by PCR–RFLP was performed with restriction enzyme *Mbo*I. The N141I mutation results in fragments of 102, 58 and 43 bp, whereas the control has fragment lengths of 102 and 58 bp. (**C**) Both PS1 and PS2 iPSC lines exhibit markers of pluripotency. All iPSCs express pluripotency markers including Tra-1-60, Tra-1-81, SSEA3 and SSEA4. Nuclei were stained with 4,6-diamidino-2-phenylindole (DAPI). Bar = 200 μm. (**D**) RT–PCR analysis of the transgenes OCT3/4, SOX2, KLF4 and the endogenous hESC marker genes. Patient fibroblasts 6 days after the transduction with the retroviruses are positive for the transgenes.

potent γ-secretase inhibitor (27) (Fig. 5A and B). With the addition of 10 and 100 nM Compound E, the production of both Aβ42 and Aβ40 was suppressed in a dose-dependent manner, when compared with untreated in both of PS1-4 and PS2-2 iPSC-derived neurons. Next, we assessed the ability of Compound W, a selective Aβ42-lowering agent, to modulate γ-secretase-mediated APP cleavage (28) (Fig. 5A and B). As expected, the addition of Compound W caused a drastic decrease in the ratio of Aβ42 to Aβ40 in both neurons.

We also determined the effect of these compounds on the proteolytic processing that causes a release of an intracellular domain of Notch, another γ-secretase substrate. Western blotting using the anti-S3 cleaved Notch1-specific antibody demonstrated that productions of Notch intracellular domain

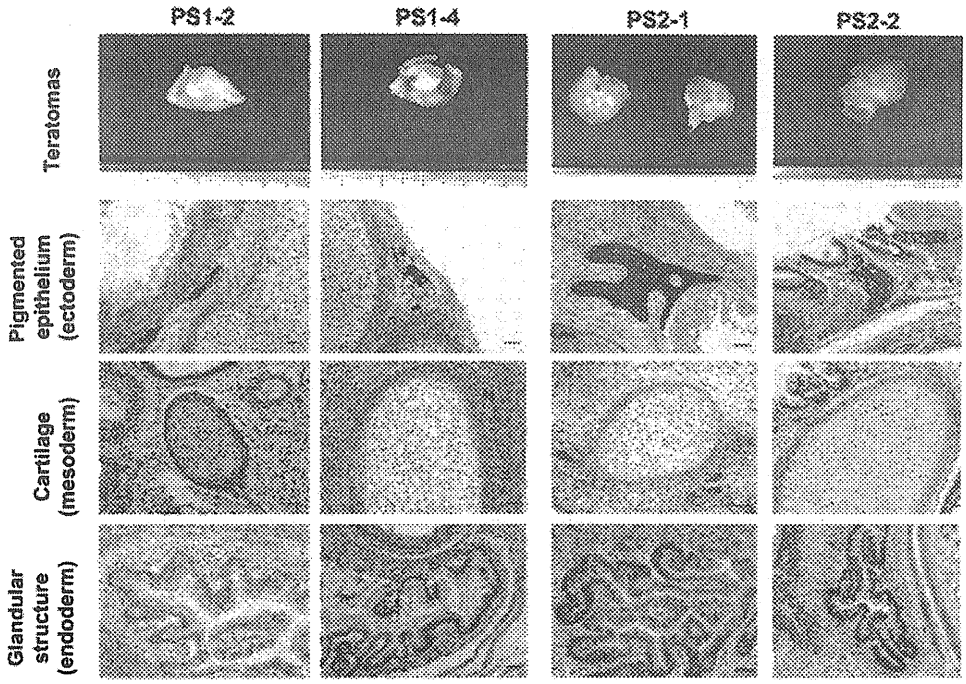

Figure 2. Teratomas derived from SCID mice injected with PS1 and PS2 iPSCs. Gross morphology, hematoxylin and eosin stained representative teratoma generated from PS 1 (PS1-2 iPSC and PS1-4 iPSC) and PS2-1 iPSC (PS2-1 iPSC and PS2-2 iPSC). Both iPSC shows tissues representing all three embryonic germ layers, including pigmented epithelium (ectoderm), cartilage (mesoderm) and glandular structure (endoderm). Bar = 50 μm.

(NICD) from both PS1-4 and PS2-2 iPSCs-derived neurons exposed to Compound E was inhibited in a dose-dependent manner. Although high dose (100 μM) of Compound W seemed to decrease NICD production in PS1-4, both neurons exposed to Compound W showed that NICD was mostly maintained (Fig. 5C). Taken together, these data indicate that both PS1 and PS2 iPSC-derived neurons respond to drug treatment in an expected manner and might be useful for drug screening in AD.

DISCUSSION

To the best of our knowledge, this study is the first to demonstrate a model of FAD using the iPSC technology. Using human neurons carrying a *PS1* mutation and a *PS2* mutation, we observed an elevation of the ratio of Aβ42 to Aβ40, a hallmark feature of FAD with presenilin mutations, in neurons derived from two clones of PS1 and PS2 iPSCs, when compared with non-AD controls (201B7, PD01-25 and 26) (Fig. 4). Although an increase in Aβ42 levels as a result of the A246E mutation in *PS1* and N141I mutation in *PS2* has been reported in patient-derived fibroblasts (11), the present study provided the first evidence of increased Aβ42 secretion by living human neurons derived from AD patients, thereby directly supporting the amyloid cascade hypothesis. To test the possibility of using the iPSC technology for drug screening, we checked the pharmacological responses to a known γ-secretase inhibitor and modulator (Fig. 5A and B). Results showed that Aβ secretion by adding agents against γ-secretase were inhibited or modulated as expected. Moreover, the Notch signaling pathway reacted with proteolytic cleavage in the presence of γ-secretase inhibitors (Fig. 5C). Recent studies have revealed that γ secretase activity is influenced in a complex manner by several cellular factors, including rafts, trafficking, expression levels of CD147, numb and gamma-secretase activating protein (1,2,29–31). We therefore propose that living human neurons from patients, i.e. FAD-iPSC-derived neurons, are very suitable material for drug development and validation of new drugs.

Previous studies on patient-specific iPSC models have mostly been limited to genetic congenital disorders (19,20,22,24,32–35). Congenital disorders may be suitable for modeling disease-specific phenotypes in the iPSC technology, because differentiated cells generated from iPSC could represent the developmental stages of disease (36). However, modeling familial PD using iPSC that carry the p.G2019S mutation in the Leucine-Rich Repeat Kinase-2 (LRRK2) gene has been reported recently (23). DA neurons derived from G2019S-iPSCs were vulnerable to exposure to stress agents, such as hydrogen peroxide, MG-132 and 6-hydroxydopamine. Now we also demonstrate the possibility of modeling the most common aging-related neurodegenerative disorder, AD, by recapitulating the key pathological mechanism (Fig. 4). Many insights into the molecular pathogenesis in neurodegenerative diseases have come from investigating post-mortem brain tissues or transgenic animals, due to the difficulty of invasive access to the living human central nervous system. With disease modeling using the iPSC technology, these new tools will make it possible to analyze living disease-specific

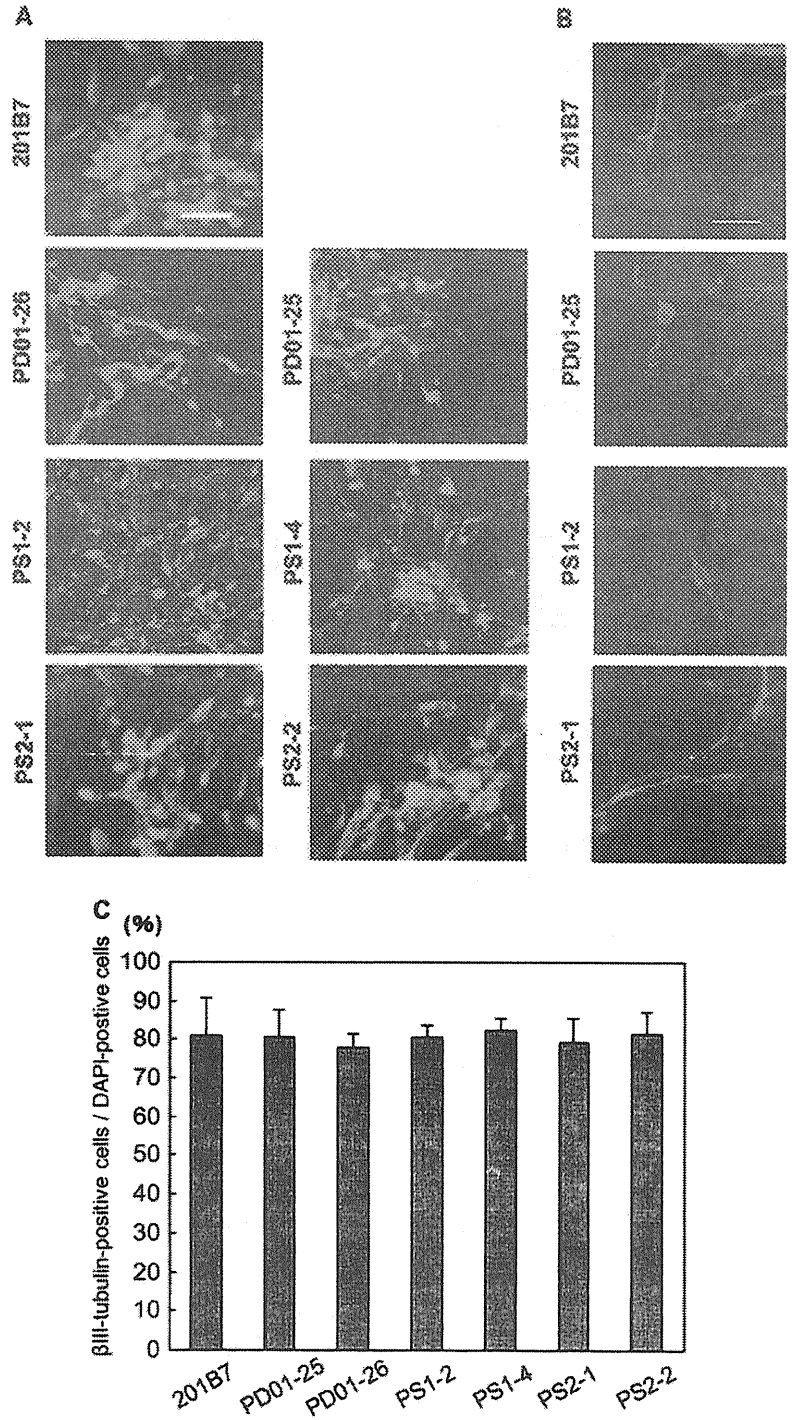

Figure 3. Differentiation of PS1 and PS2 iPSC into neurons. (**A** and **B**) Neural differentiation of control iPSC (201B7, PD01-25 and PD01-26), PS1 iPSC (PS1-2 iPSC and PS1-4 iPSC) and PS2 iPSC (PS2-1 iPSC and PS2-2 iPSC). Representative pictures of immunocytochemistry for βIII-tubulin (A) and MAP-2 (B) after neural differentiation. Bar = 40 μm (A) and 20 μm (B). (**C**) Graphs indicate the percentage of βIII-tubulin-positive cells relative to cells with DAPI-staining nuclei. Error bars indicate the SD ($n = 3$).

neurons *in vitro*. Moreover, we could graft disease-specific neurons derived from iPSCs into the brain of immunodeficient animals and we could investigate the time-dependent pathological changes *in vivo* in future studies.

FAD iPSCs could be a potential strategy for drug discovery against AD as described here; however, several limitations must be addressed in future studies. First, a high-yield of differentiated neurons from human iPSCs requires multistep

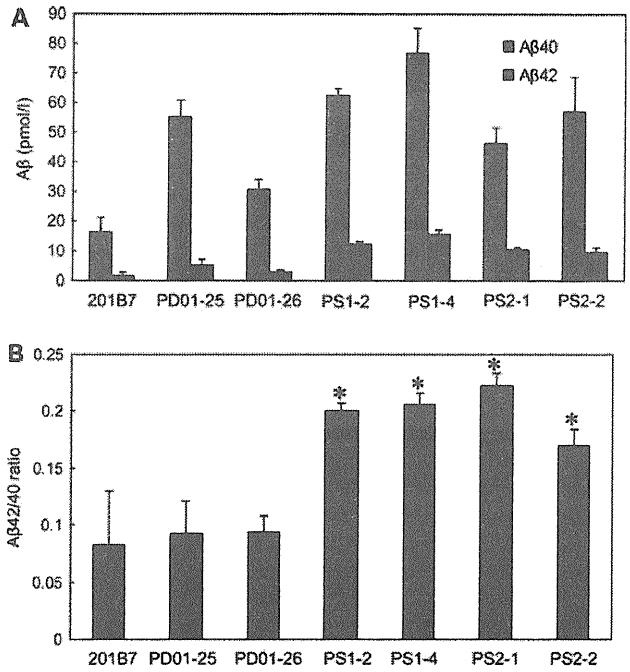

Figure 4. Characterization of Aβ secretion in PS1 and PS2 iPSC-derived neurons. (**A**) The amount of Aβ40 and Aβ42 secreted from control iPSC-derived neurons, PS1 iPSC (PS1-2 iPSC and PS1-4 iPSC) and PS2 iPSC (PS2-1 iPSC and PS2-2 iPSC)-derived neurons. (**B**) The ratio of Aβ42/Aβ40 from control iPSC-derived neurons, PS1 iPSC-derived neurons and PS2 iPSC-derived neurons. Note, the ratio of Aβ42/Aβ40 in both PS1 iPSC-derived neurons and PS2 iPSC-derived neurons was significantly higher than that of control iPSC-derived neurons. Significant differences among groups were examined by Student's *t*-test versus the ratio of 201B7 iPSC-derived neurons ($^*P < 0.05$).

procedures and prolonged culture. Furthermore, heterogeneity of differentiated neuronal cell types depending on clonal variability and culture conditions is inevitable using current differentiation methods. Clonal variation in their characters, including differentiation efficiency and tumor formation, has been a problem that needed to be solved thus far (26,37,38). Development of reliable protocols for more rapid neuronal differentiation with minimal clonal variation will be necessary, if drug discovery using iPSCs is to be fruitful. Secondly, another defining pathology in AD is an accumulation of hyperphosphorylated tau forming paired helical filaments. Growing evidence reveals that toxic Aβ directly induces tau hyperphosphorylation and accumulation, leading to neurodegeneration processes in affected neurons in AD (39,40). Pathological observations reveal that tau aggregates, but not amyloid deposits, actually correlate with dementia severity and extent of neuronal loss (41,42). Therefore, whether FAD iPSC-derived neurons exhibit accumulation of phosphorylated tau during extended culture periods should be addressed, and future studies must also focus on the biochemical dynamics of tau protein in iPSC-derived neurons treated with exogenous Aβ. Thirdly, the pathological mechanism of late-onset AD, sporadic AD and AD harboring the apoE4 allele remains unclear. Recent studies propose that impaired clearance of Aβ may cause late-onset AD through interactions with ApoE4, rather than increased Aβ production (43,44). Late-onset AD is more common and accounts for 90% of people suffering with Alzheimer's disease. To establish therapeutic strategies targeting the common form of AD, neurons derived from patient-specific iPSCs should be applied to investigations into the mechanisms underlying Aβ clearance.

Recently, a number of clinical trials of drugs targeting the pathogenesis of AD have reportedly failed in succession. Although future advances in iPSC methods are necessary for the pharmacological development and clinical application of iPSCs in neurodegeneration, we hope that our study will contribute significantly towards the identification and validation of novel candidate drugs against one of the most common and intractable diseases, AD.

MATERIALS AND METHODS

Cell culture and iPS generation

PS1 A246E fibroblasts (AG07768) and *PS2* N141I fibroblasts (AG09908) were obtained from Coriell Cell Repository. Human fibroblasts were cultured in Dulbecco's Modified Eagle's Medium (DMEM; Gibco) containing 10% fetal bovine serum, 50 U/ml penicillin, 50 mg/ml streptomycin and 1 mM L-glutamine. PS1 iPSC and PS2 iPSC were generated using the Human iPS Cell Generation Vector Set (TAKARA). G3T-hi cells were transfected with the Human iPS Cell Generation Vector set (pDON-5 OCT3/4-SOX2, pDON-5 KLF4, pDON-5 LIN28-NANOG) and pGP Vector and pE-ampho Vector with TransIT-293. Forty-eight hours after transfection, the medium (virus-containing supernatant) was collected and filtered through a 0.45 mM pore-size cellulose acetate filter. Next, the retrovirus-containing supernatant was added to RetroNectin-coated plates for centrifugation at 32°C and 2000*g* for 2 h to facilitate attachment of the virus particles onto the RetroNectin. Following this, fibroblasts were added to the plate and retrovirally transduced. Six days after transduction, fibroblasts were harvested by trypsinization and replated at 1×10^5 cells per 100 mM dish on mitomycin C-inactivated SNL cells, and the medium was changed to hiPSC medium, which consisted of DMEM/F12 medium (Invitrogen) supplemented with 20% Knock-out Serum Replacement (Invitrogen), 1 mM L-glutamine, 1 mM non-essential amino acids, 0.1 mM β-mercaptoethanol, 50 U penicillin, 50 mg/ml streptomycin (Invitrogen) and 4 ng/ml basic fibroblast growth factor (bFGF; WAKO Pure Chemicals). The hiPSC medium was changed every other day until colonies were picked. The generated iPSCs were maintained on mitomycin C-inactivated SNL cells. The hiPSC-culture medium was changed every other day, and the cells were passaged using CTK solution every 6–7 days.

Sporadic PD patient fibroblasts were generated from dermal biopsies following informed consent under protocols approved by Keio University. Two neurologists diagnosed the patient with sporadic PD, AD was excluded. Sporadic PD-derived iPSCs were generated as reported previously (14).

Reverse transcriptase-polymerase chain reaction

Total RNA samples were isolated using RNeasy (Qiagen), according to the manufacturer's instructions. The concentration

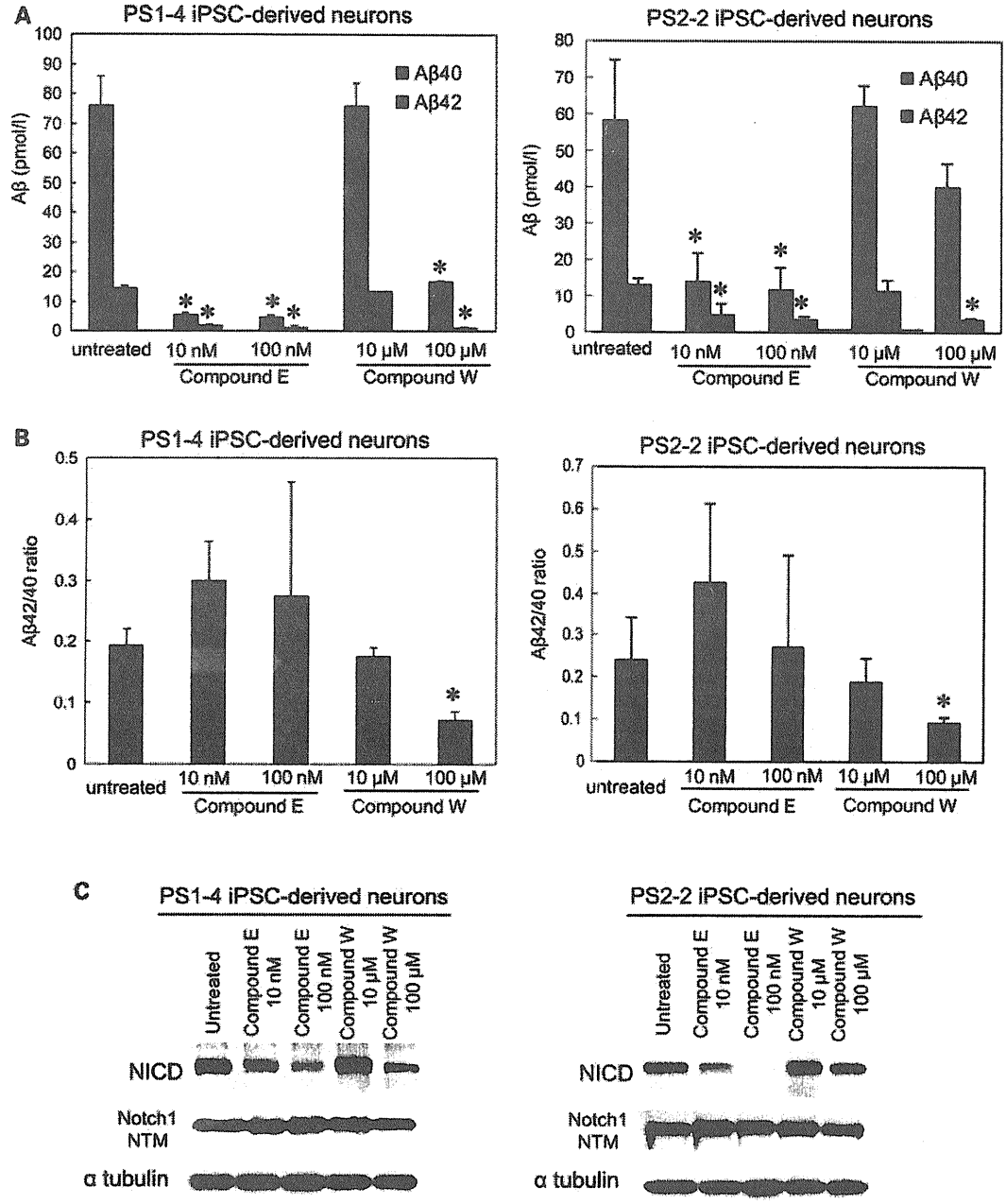

Figure 5. Pharmacological response to γ-secretase inhibitors in PS1 and PS2 iPSC-derived neurons. (**A**) The amount of Aβ40 and Aβ42 secreted from PS1-4 iPSC-derived neurons (left graph) and PS2-2 iPSC-derived neurons (right graph) treated with Compound E or W. Significant differences were examined by Student's *t*-test versus Aβ40 or Aβ42 of untreated, respectively (*$P < 0.05$). (**B**) The ratio of Aβ42/Aβ40 from PS1-4 iPSC-derived neurons (left) and PS2-2 iPSC-derived neurons (right). Significant differences were examined by Student's *t*-test versus the ratio of untreated (*$P < 0.05$). (**C**) Western blotting of S3 cleaved NICD (~110 kDa) and uncleaved Notch1 transmembrane subunit (~120 kDa) in PS1-4 iPSC-derived neurons (left) and PS2-2 iPSC-derived neurons (right) exposed to Compound E or W. α-Tubulin served as internal loading controls. Error bars in (A–D) indicate SD from three independent experiments.

and purity of the RNA was determined using the ND-1000 spectrophotometer (Nanodrop). The cDNA was synthesized using the SuperscriptIII First-Strand Synthesis System (Invitrogen). The transgene primers used in the PCR are listed in Supplementary Material, Table S2. The endogenous primers have been described previously (14).

Immunofluorescence staining of iPS and iPSC-derived differentiated neurons

Immunofluorescence staining was performed using the following primary antibodies: anti-SSEA 3 (Abcam), anti-SSEA 4 (Abcam), anti-Tra-1-60 (Millipore), anti-Tra-1-81 (Millipore),

anti-SSEA1 (Abcam), anti- MAP-2 (Chemicon) and anti-tau (HT7, Thermoscientific). 4,6-Diamidino-2-phenylindole (DAPI; Molecular Probes) was used for nuclear staining. The secondary antibodies used were: anti-rat IgG and anti-mouse IgG, and IgM conjugated with Alexa Fluor 488 or Alexa Fluor 568 (Molecular Probes).

Microarray analysis

Human genome U133 Plus 2.0 GeneChip arrays carrying 54 690 probe sets (Affymetrix) were used for microarray hybridizations to examine global gene expression. Approximately 150 ng of RNA from each sample was labeled using GeneChip 3′IVT Express (Affymetrix) according to the manufacturer's instructions. All arrays were hybridized at 45°C for 16 h and scanned using an AFX GC3000 G7 scanner. The gene expression raw data were extracted using the AFX Gene Chip Operation System. Quality control was performed on the basis of Affymetrix quality control metrics. The data were analyzed with the Gene Spring GX 11.0 (Agilent). Two normalization procedures were applied. Initially, the signal intensities with values <0.1 were assigned a value of 0.1. Then, each chip was normalized to the 50th percentile of the measurements taken from that chip. Each gene was normalized to the median of that gene in the respective controls, to enable comparisons of relative changes in gene expression levels between different conditions.

Microarray data can be found at the GEO website under accession number 'GSE28379'. (The following link has been created to allow review of record GSE28379: http://www.ncbi.nlm.nih.gov/geo/query/acc.cgi?token=zlovzkaqqwugkdg&acc=GSE28379.) The gene expression profiles of BJ fibroblasts (GSM248214) were downloaded from the NCBI Gene Expression Omnibus (GEO) database.

aCGH analysis

Genomic DNA was isolated using DNeasy (Qiagen), according to the manufacturer's instructions. DNA concentrations were measured on a Nanodrop ND-1000 spectrophotometer (Isogen). DNA quality was monitored with the Agilent 2100 Bioanalyzer (Agilent Technologies). DNA (500 ng) was labeled using the Enzo Genomic DNA Labeling kit. Hybridizations were performed on slides containing four arrays, with each array containing 622 060 *in situ* synthesized 60-mer oligonucleotides, representing 170 344 unique chromosomal locations (Agilent Technologies). Images of the arrays were acquired using a microarray scanner G2505CA (Agilent technologies) and image analysis was performed using feature extraction software version 10.7 (Agilent Technologies). The Agilent CGH-v4_107_Sep09 protocol was applied using default settings. Oligonucleotides were mapped according to the human genome build NCBI 36. The obtained data were imported into Agilent Genomic Workbench using the aberration detection method 2 (ADM-2) algorithm (10.0 threshold) for further analysis. The aCGH data have been deposited in GEO and given the series accession number GSE28450. (The following link has been created to allow review of record GSE28450: http://www.ncbi.nlm.nih.gov/geo/query/acc.cgi?token=ntsvfkqkucksgrc&acc=GSE28450.)

In vitro differentiation

Cells were harvested using CTK solutions and a cell scraper, and transferred to a Petri dish in hiPSC medium without bFGF to form embryoid bodies. After 8 days, embryoid bodies were plated onto gelatin-coated tissue culture dishes and incubated for an additional 8 days. The cells were incubated at 37°C in 5% CO_2 and the medium was replaced every other day. The cells were stained with mouse anti-α-fetoprotein IgG (R&D Systems), anti-smooth muscle actin (Sigma), anti-βIII-tubulin mouse IgG (Chemicon), together with DAPI.

Teratoma formation

hiPSCs were injected into the subcutaneous tissue of SCID mice (CREA). At 8–10 weeks post-injection, teratomas were dissected, fixed in 10% formaldehyde in PBS and embedded in paraffin.

Neural induction

Neural induction of hiPSCs cells was performed as previously described with slight modifications (Okada *et al.*, in preparation) (25,26). For terminal differentiation, induced neural cells were plated onto Matrigel-coated coverslips and cultured for 2 weeks. This was followed by the addition of Compound E, 2S-2-{[(3,5-difluorophenyl)acetyl]amino}-*N*-[(3S)-1-methyl-2-oxo-5-phenyl-2,3-dihydro-1H-1,4-benzodiazepin-3-yl]propanamide (Calbiochem) or Compound W, 3,5-Bis(4-nitrophenoxy)benzoic Acid (Tokyo Chemical Industry) for 48 h.

Quantitation of Aβ by ELISA

Conditioned media of differentiated neurons were collected after an incubation period of 48 h and subjected to β Amyloid ELISA Kits (WAKO), according to the manufacturer's instructions.

Immunoblot analysis

Cells were briefly sonicated in cold lysis buffer (50 mM Tris–HCl, pH 7.4, 150 mM NaCl, 0.5% NP-40, 0.5% sodium deoxycholate, 0.25% sodium dodecyl sulfate, 5 mM EDTA and protease inhibitor cocktail from Sigma). Total protein concentration in the supernatant was determined using a Bio-Rad protein assay kit. The proteins were then analyzed by immunoblotting as follows: protein samples were separated by reducing SDS–PAGE on a 4–20% Tris–glycine gradient gel (Invitrogen), and then transferred to a polyvinylidene difluoride membrane (Millipore). The membrane was incubated with primary antibodies and then horseradish peroxidase-conjugated secondary antibodies. Detection was performed using enhanced chemiluminescence reagents as described by the supplier (PerkinElmer Life Sciences). Primary monoclonal antibodies that were used in this study were: anti-tau (HT7, Thermoscientific), anti-NICD (Cell Signaling Technology), anti-Notch1 (D1E11) (Cell Signaling Technology) and alpha tubulin (Cell Signaling Technology).

Statistical analysis

Statistical analysis of the data was performed by Student's *t*-test using JMP 8 (SAS Institute, Inc.).

SUPPLEMENTARY MATERIAL

Supplementary Material is available at *HMG* online.

ACKNOWLEDGEMENTS

T.Y. is a research fellow of the Japan Society for the Promotion of Science. This work was supported by grants from Eisai Co. Ltd (to D.I. and N.S.) and the project for realization of regenerative medicine from the Ministry of Education, Culture, Sports, Science and Technology of Japan to H.O. We thank Mari Fujiwara (Core Instrumentation Facility, Keio University School of Medicine) for the microarray analysis and Satoko Iwasawa (Department of Preventive Medicine and Public Health, School of Medicine, Keio University) for helpful advice about statistical analysis. We also thank Dr Xu Huaxi for providing the T44 Tau pSG5 plasmid (Sanford-Burnham Medical Research Institute).

Conflict of Interest statement. None declared.

FUNDING

This work was supported by grants from Eisai Co. Ltd (to D.I. and N.S.), the Research Fellowship grant of the Japan Society for the Promotion of Science (to T.Y.), and the Project for Realization of Regenerative Medicine, and Support for Core Institutes for iPS Cell Research from the Ministry of Education, Culture, Sports, Science and Technology of Japan (to H.O.).

REFERENCES

1. Vetrivel, K.S. and Thinakaran, G. (2006) Amyloidogenic processing of beta-amyloid precursor protein in intracellular compartments. *Neurology*, **66**, S69–S73.
2. Thinakaran, G. and Koo, E.H. (2008) Amyloid precursor protein trafficking, processing, and function. *J. Biol. Chem.*, **283**, 29615–29619.
3. Hardy, J. and Selkoe, D.J. (2002) The amyloid hypothesis of Alzheimer's disease: progress and problems on the road to therapeutics. *Science*, **297**, 353–356.
4. Tanzi, R.E. and Bertram, L. (2005) Twenty years of the Alzheimer's disease amyloid hypothesis: a genetic perspective. *Cell*, **120**, 545–55.
5. Sisodia, S.S. and St George-Hyslop, P.H. (2002) gamma-Secretase, Notch, Abeta and Alzheimer's disease: where do the presenilins fit in? *Nat. Rev. Neurosci.*, **3**, 281–290.
6. Sherrington, R., Rogaev, E.I., Liang, Y., Rogaeva, E.A., Levesque, G., Ikeda, M., Chi, H., Lin, C., Li, G., Holman, K. *et al.* (1995) Cloning of a gene bearing missense mutations in early-onset familial Alzheimer's disease. *Nature*, **375**, 754–760.
7. Cruts, M., van Duijn, C.M., Backhovens, H., Van den Broeck, M., Wehnert, A., Serneels, S., Sherrington, R., Hutton, M., Hardy, J., St George-Hyslop, P.H. *et al.* (1998) Estimation of the genetic contribution of presenilin-1 and -2 mutations in a population-based study of presenile Alzheimer disease. *Hum. Mol. Genet.*, **7**, 43–51.
8. Levy-Lahad, E., Wasco, W., Poorkaj, P., Romano, D.M., Oshima, J., Pettingell, W.H., Yu, C.E., Jondro, P.D., Schmidt, S.D., Wang, K. *et al.* (1995) Candidate gene for the chromosome 1 familial Alzheimer's disease locus. *Science*, **269**, 973–977.
9. Jayadev, S., Leverenz, J.B., Steinbart, E., Stahl, J., Klunk, W., Yu, C.E. and Bird, T.D. (2010) Alzheimer's disease phenotypes and genotypes associated with mutations in presenilin 2. *Brain*, **133**, 1143–1154.
10. Borchelt, D.R., Thinakaran, G., Eckman, C.B., Lee, M.K., Davenport, F., Ratovitsky, T., Prada, C.M., Kim, G., Seekins, S., Yager, D. *et al.* (1996) Familial Alzheimer's disease-linked Presenilin 1 variants elevate Aβ1-42/1-40 ratio in vitro and in vivo. *Neuron*, **17**, 1005–1013.
11. Scheuner, D., Eckman, C., Jensen, M., Song, X., Citron, M., Suzuki, N., Bird, T.D., Hardy, J., Hutton, M., Kukull, W. *et al.* (1996) Secreted amyloid β-protein similar to that in the senile plaques of Alzheimer's disease is increased in vivo by the presenilin 1 and 2 and APP mutations linked to familial Alzheimer's disease. *Nat. Med.*, **2**, 864–870.
12. Tomita, T., Maruyama, K., Saido, T.C., Kume, H., Shinozaki, K., Tokuhiro, S., Capell, A., Walter, J., Grünberg, J., Haass, C. *et al.* (1997) The presenilin 2 mutation (N141I) linked to familial Alzheimer disease (Volga German families) increases the secretion of amyloid beta protein ending at the 42nd (or 43rd) residue. *Proc. Natl Acad. Sci. USA*, **94**, 2025–2030.
13. Oyama, F., Sawamura, N., Kobayashi, K., Morishima-Kawashima, M., Kuramochi, T., Ito, M., Tomita, T., Maruyama, K., Saido, T.C., Iwatsubo, T. *et al.* (1998) Mutant presenilin 2 transgenic mouse: effect on an age-dependent increase of amyloid beta-protein 42 in the brain. *J. Neurochem.*, **71**, 313–322.
14. Takahashi, K., Tanabe, K., Ohnuki, M., Narita, M., Ichisaka, T., Tomoda, K. and Yamanaka, S. (2007) Induction of pluripotent stem cells from adult human fibroblasts by defined factors. *Cell*, **131**, 861–872.
15. Yu, J., Vodyanik, M.A., Smuga-Otto, K., Antosiewicz-Bourget, J., Frane, J.L., Tian, S., Nie, J., Jonsdottir, G.A., Ruotti, V., Stewart, R. *et al.* (2007) Induced pluripotent stem cell lines derived from human somatic cells. *Science*, **318**, 1917–1920.
16. Dimos, J.T., Rodolfa, K.T., Niakan, K.K., Weisenthal, L.M., Mitsumoto, H., Chung, W., Croft, G.F., Saphier, G., Leibel, R., Goland, R. *et al.* (2008) Induced pluripotent stem cells generated from patients with ALS can be differentiated into motor neurons. *Science*, **321**, 1218–1221.
17. Park, I.H., Arora, N., Huo, H., Maherali, N., Ahfeldt, T., Shimamura, A., Lensch, M.W., Cowan, C., Hochedlinger, K. and Daley, G.Q. (2008) Disease-specific induced pluripotent stem cells. *Cell*, **134**, 877–886.
18. Soldner, F., Hockemeyer, D., Beard, C., Gao, Q., Bell, G.W., Cook, E.G., Hargus, G., Blak, A., Cooper, O., Mitalipova, M. *et al.* (2009) Parkinson's disease patient-derived induced pluripotent stem cells free of viral reprogramming factors. *Cell*, **136**, 964–977.
19. Ebert, A.D., Yu, J., Rose, F.F. Jr., Mattis, V.B., Lorson, C.L., Thomson, J.A. and Svendsen, C.N. (2009) Induced pluripotent stem cells from a spinal muscular atrophy patient. *Nature*, **457**, 277–280.
20. Lee, G., Papapetrou, E.P., Kim, H., Chambers, S.M., Tomishima, M.J., Fasano, C.A., Ganat, Y.M., Menon, J., Shimizu, F., Viale, A. *et al.* (2009) Modelling pathogenesis and treatment of familial dysautonomia using patient-specific iPSCs. *Nature*, **461**, 402–406.
21. Ku, S., Soragni, E., Campau, E., Thomas, E.A., Altun, G., Laurent, L.C., Loring, J.F., Napierala, M. and Gottesfeld, J.M. (2010) Friedreich's ataxia induced pluripotent stem cells model intergenerational GAA TTC triplet repeat instability. *Cell Stem Cell*, **7**, 631–637.
22. Chamberlain, S.J., Chen, P.F., Ng, K.Y., Bourgois-Rocha, F., Lemtiri-Chlieh, F., Levine, E.S. and Lalande, M. (2010) Induced pluripotent stem cell models of the genomic imprinting disorders Angelman and Prader-Willi syndromes. *Proc. Natl Acad. Sci. USA*, **107**, 17668–17673.
23. Nguyen, H.N., Byers, B., Cord, B., Shcheglovitov, A., Byrne, J., Gujar, P., Kee, K., Schüle, B., Dolmetsch, R.E., Langston, W. *et al.* (2011) LRRK2 mutant iPSC-derived DA neurons demonstrate increased susceptibility to oxidative stress. *Cell Stem Cell*, **8**, 267–280.
24. Marchetto, M.C., Carromeu, C., Acab, A., Yu, D., Yeo, G.W., Mu, Y., Chen, G., Gage, F.H. and Muotri, A.R. (2010) A model for neural development and treatment of Rett syndrome using human induced pluripotent stem cells. *Cell*, **143**, 527–539.
25. Okada, Y., Matsumoto, A., Shimazaki, T., Enoki, R., Koizumi, A., Ishii, S., Itoyama, Y., Sobue, G. and Okano, H. (2008) Spatiotemporal recapitulation of central nervous system development by murine embryonic stem cell-derived neural stem/progenitor cells. *Stem Cells*, **26**, 3086–3098.
26. Miura, K., Okada, Y., Aoi, T., Okada, A., Takahashi, K., Okita, K., Nakagawa, M., Koyanagi, M., Tanabe, K., Ohnuki, M. *et al.* (2009)

Variation in the safety of induced pluripotent stem cell lines. *Nat. Biotechnol.*, **27**, 743–745.
27. Beher, D., Wrigley, J.D., Nadin, A., Evin, G., Masters, C.L., Harrison, T., Castro, J.L. and Shearman, M.S. (2001) Pharmacological knock-down of the presenilin 1 heterodimer by a novel gamma-secretase inhibitor: implications for presenilin biology. *J. Biol. Chem.*, **276**, 45394–45402.
28. Okochi, M., Fukumori, A., Jiang, J., Itoh, N., Kimura, R., Steiner, H., Haass, C., Tagami, S. and Takeda, M. (2006) Secretion of the Notch-1 Abeta-like peptide during Notch signaling. *J. Biol. Chem.*, **281**, 7890–7898.
29. Zhou, S., Zhou, H., Walian, P.J. and Jap, B.K. (2005) CD147 is a regulatory subunit of the gamma-secretase complex in Alzheimer's disease amyloid beta-peptide production. *Proc. Natl Acad. Sci. USA*, **102**, 7499–7504.
30. He, G., Luo, W., Li, P., Remmers, C., Netzer, W.J., Hendrick, J., Bettayeb, K., Flajolet, M., Gorelick, F., Wennogle, L.P. *et al.* (2010) Gamma-secretase activating protein is a therapeutic target for Alzheimer's disease. *Nature*, **467**, 95–98.
31. Kyriazis, G.A., Wei, Z., Vandermey, M., Jo, D.G., Xin, O., Mattson, M.P. and Chan, S.L. (2008) Numb endocytic adapter proteins regulate the transport and processing of the amyloid precursor protein in an isoform-dependent manner: implications for Alzheimer disease pathogenesis. *J. Biol. Chem.*, **283**, 25492–25502.
32. Liu, G.H., Barkho, B.Z., Ruiz, S., Diep, D., Qu, J., Yang, S.L., Panopoulos, A.D., Suzuki, K., Kurian, L., Walsh, C. *et al.* (2011) Recapitulation of premature ageing with iPSCs from Hutchinson–Gilford progeria syndrome. *Nature*, **472**, 221–225.
33. Zhang, J., Lian, Q., Zhu, G., Zhou, F., Sui, L., Tan, C., Mutalif, R.A., Navasankari, R., Zhang, Y., Tse, H.F. *et al.* (2011) A human iPSC model of Hutchinson Gilford progeria reveals vascular smooth muscle and mesenchymal stem cell defects. *Cell Stem Cell*, **8**, 31–45.
34. Yazawa, M., Hsueh, B., Jia, X., Pasca, A.M., Bernstein, J.A., Hallmayer, J. and Dolmetsch, R.E. (2011) Using induced pluripotent stem cells to investigate cardiac phenotypes in Timothy syndrome. *Nature*, **471**, 230–234.
35. Carvajal-Vergara, X., Sevilla, A., D'Souza, S.L., Ang, Y.S., Schaniel, C., Lee, D.F., Yang, L., Kaplan, A.D., Adler, E.D., Rozov, R. *et al.* (2010) Patient-specific induced pluripotent stem-cell-derived models of LEOPARD syndrome. *Nature*, **465**, 808–812.
36. Mattis, V.B. and Svendsen, C.N. (2011) Induced pluripotent stem cells: a new revolution for clinical neurology? *Lancet Neurol.*, **10**, 383–394.
37. Hu, B.Y., Weick, J.P., Yu, J., Ma, L.X., Zhang, X.Q., Thomson, J.A. and Zhang, S.C. (2010) Neural differentiation of human induced pluripotent stem cells follows developmental principles but with variable potency. *Proc. Natl Acad. Sci. USA*, **107**, 4335–5340.
38. Boulting, G.L., Kiskinis, E., Croft, G.F., Amoroso, M.W., Oakley, D.H., Wainger, B.J., Williams, D.J., Kahler, D.J., Yamaki, M., Davidow, L. *et al.* (2011) A functionally characterized test set of human induced pluripotent stem cells. *Nat. Biotechnol.*, **29**, 279–286.
39. Busciglio, J., Lorenzo, A., Yeh, J. and Yankner, B.A. (1995) Beta-amyloid fibrils induce tau phosphorylation and loss of microtubule binding. *Neuron*, **14**, 879–888.
40. Jin, M., Shepardson, N., Yang, T., Chen, G., Walsh, D. and Selkoe, D.J. (2011) Soluble amyloid β-protein dimers isolated from Alzheimer cortex directly induce Tau hyperphosphorylation and neuritic degeneration. *Proc. Natl Acad. Sci. USA*, **108**, 5819–5824.
41. Bierer, L.M., Hof, P.R., Purohit, D.P., Carlin, L., Schmeidler, J., Davis, K.L. and Perl, D.P. (1995) Neocortical neurofibrillary tangles correlate with dementia severity in Alzheimer's disease. *Arch. Neurol.*, **52**, 81–88.
42. Schmitt, O., Eggers, R. and Haug, H. (1995) Quantitative investigations into the histostructural nature of the human putamen. I. Staining, cell classification and morphometry. *Ann. Anat.*, **177**, 243–250.
43. Jiang, Q., Lee, C.Y., Mandrekar, S., Wilkinson, B., Cramer, P., Zelcer, N., Mann, K., Lamb, B., Willson, T.M., Collins, J.L. *et al.* (2008) ApoE promotes the proteolytic degradation of Abeta. *Neuron*, **58**, 681–693.
44. Mawuenyega, K.G., Sigurdson, W., Ovod, V., Munsell, L., Kasten, T., Morris, J.C., Yarasheski, K.E. and Bateman, R.J. (2010) Decreased clearance of CNS beta-amyloid in Alzheimer's disease. *Science*, **330**, 1774.